Short Communication

A Simple and Effective Way to Overcome Carbon Monoxide Poisoning of Platinum Surfaces in Direct Formic Acid Fuel Cells

Islam M. Al-Akraa[*], *Yaser M. Asal, Sohair A. Darwish*

Department of Chemical Engineering, Faculty of Engineering, The British University in Egypt, Cairo 11837, Egypt
[*]E-mail: islam.ahmed@bue.edu.eg; islam0886@yahoo.com

A glassy carbon (GC) electrode modified with multi-walled carbon nanotubes (MWCNTs) and platinum nanoparticles (PtNPs), Pt/MWCNTs-GC, has been introduced for formic acid electro-oxidation (FAO). A similar loading of PtNPs has been conserved for a proper comparison between the Pt/MWCNTs-GC and the unmodified Pt/GC electrodes. The modification with MWCNTs could enhance the loading of PtNPs onto the GC electrode in a way that minimizes its agglomeration and increases its dispersion in the CNTs network. This not only increases the surface area exposed to the reaction but also interrupts the contiguity of the Pt active sites minimizing the adsorption of the poisoning CO. As a result, both of the I_p^d/I_p^{ind} and I_p^d/I_p^b ratios were increased by 12.5 and 2.5 times. Several techniques will be combined to track the catalyst activity and to determine its morphology.

1. INTRODUCTION

Nowadays, one of the biggest challenges facing the entire world is meeting the continuous increase in global energy demand [1, 2]. Traditional sources of energy can no longer provide the power needed by the modern societies, in addition, burning fossil fuels emits large harmful amounts of carbon to the atmosphere every year. For these reasons, the world has moved searching for other clean energy sources, one of which is the fuel cells (FCs) [3-5]. FCs considered green, reliable, safe, flexible, and most importantly efficient, which all make it a promising source of electricity [6-8].

One of the promising fuels could be oxidized is formic acid (FA) since it showed a huge potential environmentally, economically and technically. Also, FA showed a low crossover flux through Nafion membranes, the electrolyte typically used in direct formic acid fuel cells (DFAFCs). Because of that,

making compact portable power systems is now possible by using very concentrated FA as a fuel with ultra-thin membranes [9-11]. The strong distinct odor that FA has is considered a bonus, as any leakages would be detected early in DFAFCs. Additionally, DFAFCs have a higher open-circuit potential compared to HFCs, as the theoretical potentials are 1.40 V and 1.23 V vs. RHE, respectively [12, 13].

In order to oxidize FA in DFAFCs, Platinum-based catalysts were typically used. FA electro-oxidation at a Pt surface takes place either through a direct or an indirect pathway [14-17]. The direct pathway involves the dehydrogenation of FA molecule to CO_2 at low potential domain, hence is highly preferred. Alternatively, the indirect pathway involves the non-faradic dissociation of FA molecule generating CO as an intermediate product, which later could be oxidized at higher potential domain. The indirect pathway is not preferred because the CO generated is adsorbed at the Pt surface resulting in a surface poisoning and so a reduced catalytic performance at low potential domain [18-20].

Generally, electrocatalysis by metal/metal oxide nanostructures has been growing because of the fascinating properties of these nanostructures [21-25]. Indeed, several attempts have been carried out to overcome the problem of CO adsorption by several approaches [26-29]. In this study, a simple and a high efficient way to reduce the CO poisoning at the Pt surface and to increase its stability is proposed by modifying the GC electrode (substrate) with MWCNTs. The catalysts will be characterized electrochemically and by a scanning electron microscopy (SEM) coupled with energy dispersive X-ray spectrometer (EDS). Its activity and stability will be monitored towards FAO.

2. EXPERIMENTAL

2.1. Electrodes' preparation

The preparation of the electrocatalyst started with modifying the GC electrode with MWCNTs. First, 10 mg of MWCNTs were added to 1 ml of 5% Nafion/ethanol then sonicated for one hour. Later, 10 µL of the obtained suspension is spread evenly on the GC electrode's surface then left for an hour at room temperature to allow the ethanol to evaporate. Finally, the modified GC electrode was washed with second distilled water. Then, a 10 mC of PtNPs has been electrodeposited on the modified MWCNTs-GC electrode (the modified electrode will be abbreviated as Pt/MWCNTs-GC, that is mean that GC electrode firstly modified with MWCNTs then with PtNPs) at 0.1 V in 0.1 M Na_2SO_4 solution containing 1 mM H_2PtCl_6. For comparison, a Pt/GC electrode (GC only modified with PtNPs). A spiral Pt wire and a saturated calomel electrode (SCE) electrodes served as the counter and reference electrodes, respectively.

2.2. Electrochemical and Material characterization

The electrochemical measurements were carried out in a traditional three-electrode glass cell at room temperature (around 25 °C) using a Bio-Logic SAS potentiostat (model SP-150) operated with EC-Lab software. The catalytic performance of the modified electrodes toward FAO was investigated in 0.3 M FA solution (pH = 3.5).

A Field-emission scanning electron microscope (FE-SEM) (FEI, QUANTA FEG250, ThermoFisher) coupled with energy dispersive X-ray spectrometer (EDS) was used to evaluate the morphology of the prepared modified electrodes.

3. RESULTS AND DISCUSSION

3.1. Electrochemical and Material characterization

The electrochemical characterization is really helpful in providing all the required information about the composition of the catalyst's surface, specifically the electroactive ingredient (Pt) as well as its exposed surface area.

Figure 1 shows the cyclic voltammograms (CVs) of (a) Pt/GC and (b) Pt/MWCNTs-GC modified electrodes measured in 0.5 M H_2SO_4 at a potential scan rate of 100 mV s^{-1}.
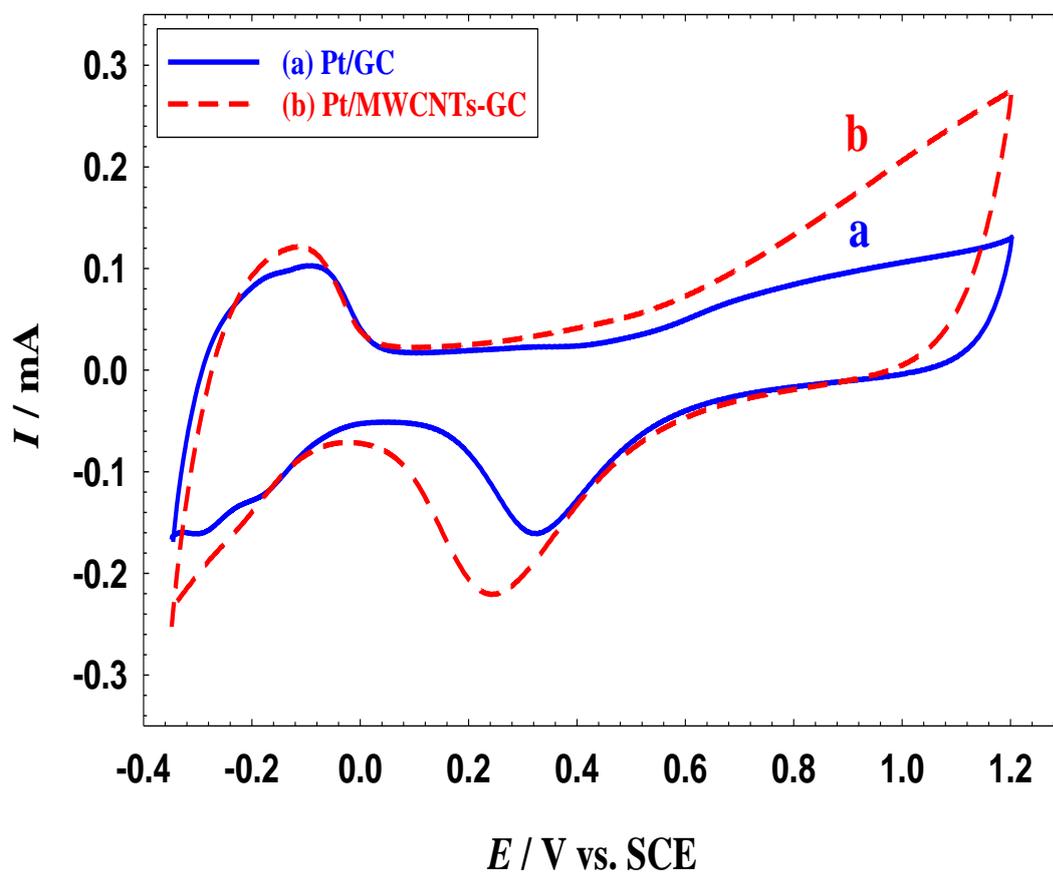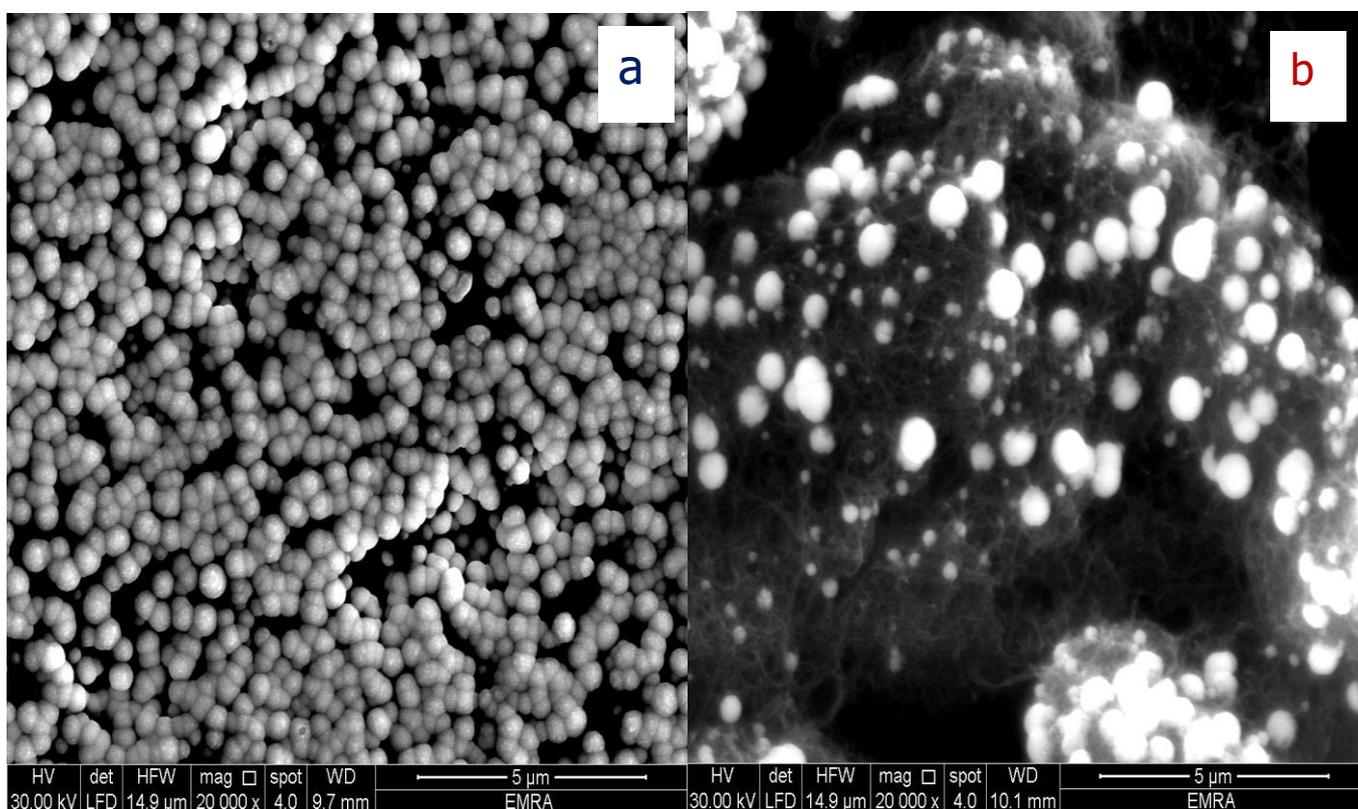

Figure 1. CVs of the (a) Pt/GC and (b) Pt/MWCNTs-GC modified electrodes measured in 0.5 M H_2SO_4 at a potential scan rate of 100 mV s^{-1}.

For both modified electrodes, the obtained CVs shown in Fig. 1 exhibit the typical characteristics of pure polycrystalline Pt electrode in an acidic medium [30, 31]. The Pt oxidation region, lies in the

range from 0.6 to 1.2 V, is coupled with a reduction peak at ca. 0.3 V corresponding to PtO reduction. Moreover, the hydrogen adsorption/desorption ($H_{ads/des}$) peaks observed in the potential range from 0.0 to − 0.3 V. By modifying the GC electrode with MWCNTs before PtNPs deposition (Pt/MWCNTs-GC, Fig. 1b), several observations have been noticed;

- Pt oxidation started from ca. 0.3 V compared with ca. 0.5 V obtained at Pt/GC electrode.
- PtO reduction peak has been shifted to a lower potential.
- Although the amount of loaded PtNPs is fixed, its surface area (A_r), calculated from the charge of the PtO reduction peak or $H_{ads/des}$ peaks, has been increased from 0.64 cm^2 at Pt/GC electrode to 0.81 cm^2 because of loading distribution within the CNTs network.

From another perspective, the surface morphology of the two modified electrodes was scanned using FE-SEM. Figure 2 represents FE-SEM micrographs for (a)Pt/GC and (b) Pt/MWCNTs-GC modified electrodes.
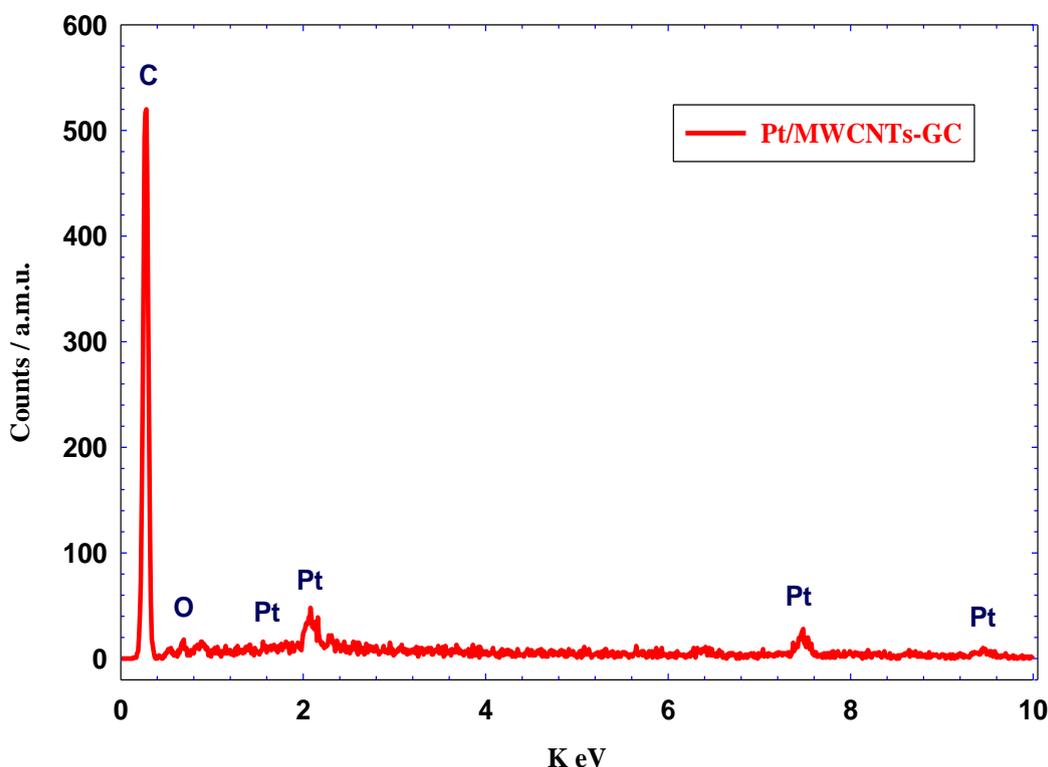

Figure 2. FE-SEM micrographs of the (a) Pt/GC and (b) Pt/MWCNTs-GC modified electrodes. The electrodeposition conditions are listed in the experimental section.

For the Pt/GC electrode (Fig. 2a) the PtNPs was electrodeposited directly on the GC electrode in spherical agglomerations with an average particle size of 150 nm. On the other hand, in the

Pt/MWCNTs-GC modified electrode (Fig. 2b), the PtNPs was electrodeposited on the MWCNTs network as non-agglomerated spherical particles with a smaller average diameter.

The EDS analysis of the catalyst (Pt/MWCNTs-GC) provided a confirmation for the deposition of all constituting ingredients in the catalyst (C, O and Pt) and further assessed their relative compositions (see Fig. 3).


Figure 3. EDS analysis of the Pt/MWCNTs-GC electrode. The electrodeposition conditions are listed in the experimental section.

3.2. Electrocatalysis of FAO

Figure 4 shows the CVs of FAO at the Pt/GC (a) and Pt/ MWCNTs-GC (b) modified electrodes in an aqueous solution of 0.3 M formic acid (pH = 3.5). Generally, the mechanism of FAO on Pt-based electrocatalysts proceeds in two different routes [32, 33] . The first one involves dehydrogenation of FA to CO_2. This direct route takes place at a low potential domain thus shifts the actual voltage of DFAFCs closer to its theoretical value. That is why this route is the preferred route for FAO. In Fig. 4, the peak observed at 0.3 V in the forward scan at the Pt/GC (a) and Pt/MWCNTs-GC (b) electrodes represents FAO through this route (represented by Eq. 1). In order to check the density of active Pt sites that have participated in the direct FAO, the corresponding current to the direct peak is used (I_p^d).

$$HCOOH_{(aq)} + Pt \rightarrow Pt + CO_{2(g)} + 2H_{(aq)}^+ + 2e^- \tag{1}$$
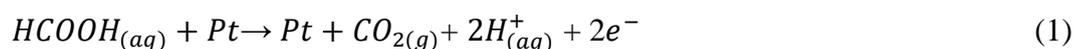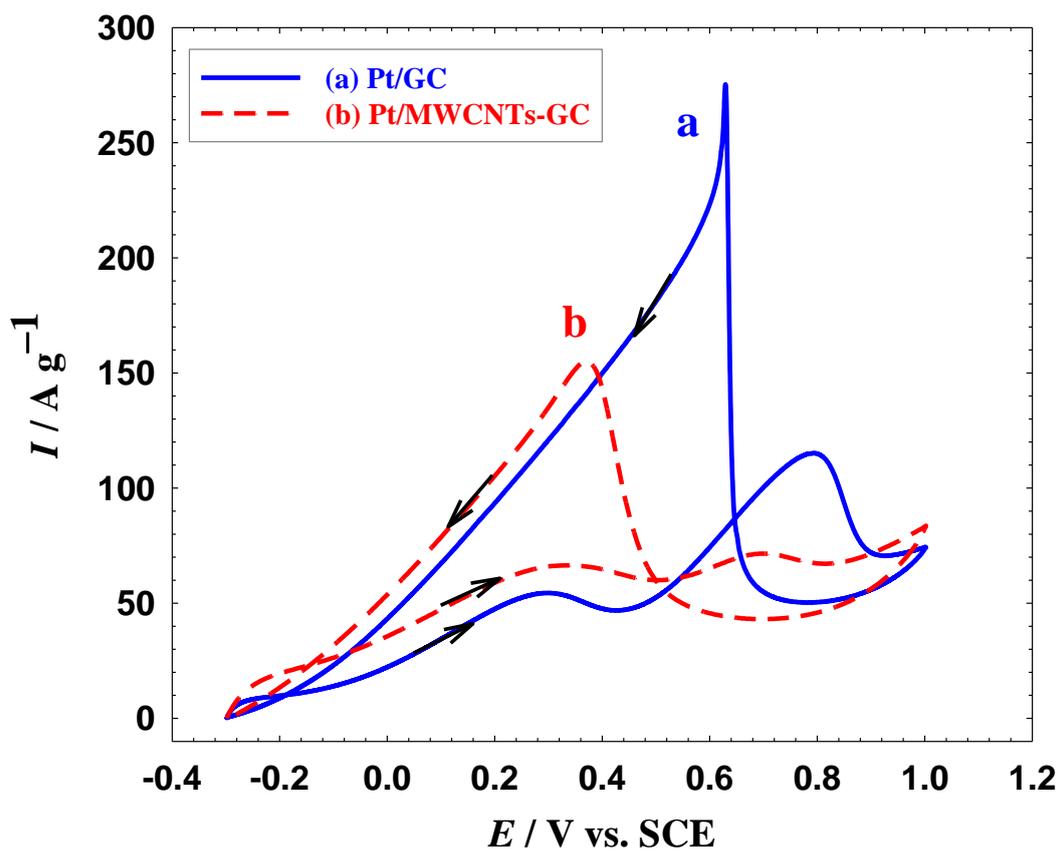
Figure 4. CVs of the (a) Pt/GC and (b) Pt/MWCNTs-GC electrodes measured in 0.3 M formic acid (pH = 3.5) at a potential scan rate of 100 mVs^{-1}.

Alternatively, FAO could proceed via CO production which blocks the Pt active sites at lower potential which explains why this route is extremely not preferred (represented by Eq. 2).

$$HCOOH + Pt \rightarrow Pt\text{–}CO_{ads} + H_2O \tag{2}$$

At higher potentials, the CO will be oxidized again to CO_2 according to equations 3 and 4 and the peak observed at ca. 0.75 V in the forward scan at the Pt/GC (a) and Pt/MWCNTs-GC (b) electrodes represents FAO through this route and the corresponding current to the indirect peak is used (I_p^{ind}).

$$Pt + H_2O \rightarrow Pt\text{–}OH + H^+ + e^- \tag{3}$$
$$Pt\text{–}CO_{ads} + Pt\text{–}OH \rightarrow 2Pt + CO_2 + H^+ + e^- \tag{4}$$
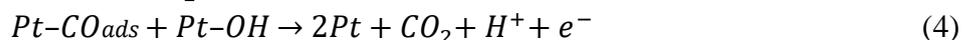
In the backward scan (cathodic scan), the majority of the adsorbed CO could be oxidized in the forward scan, thus FAO proceeds mainly through the direct route. This can be observed from the higher current of the backward scan (I_p^b).

The relative ratios of I_p^d / I_p^{ind} and I_p^d / I_p^b were calculated, respectively, in order to quantify the degree of catalytic enhancement toward FAO and the reduction in CO poisoning for both electrodes. The values of I_p^d / I_p^{ind} and I_p^d / I_p^b at the Pt/GC electrode (Fig. 4a) were 0.60 and 0.19, respectively. The main aim of this modification with MWCNTs is to increase the I_p^d /I_p^{ind} and I_p^d /I_p^b ratios to reasonable values. Figure 4b, which represents the CV of FAO on a Pt/MWCNTs-GC electrode showed how interrupting the agglomeration of the PtNPs, carried out by the loading distribution within the CNTs network, successfully enhanced the catalytic activity of the direct route of FAO, as inferred from the large increase of I_p^d and decrease of I_p^{ind} compared with that of the Pt/GC electrode, eventually improving the I_p^d / I_p^{ind} ratio from 0.60 on Pt/GC to 7.5 on Pt/MWCNTs-GC electrode (i.e., ca. 12.5 times increase). In addition, modifying the electrode with MWCNTs also significantly increased the I_p^d / I_p^b ratio from 0.19 on Pt/GC to 0.45 on Pt/MWCNTs-GC electrode (i.e., ca. 2.3 times increase); indicating a higher catalytic tolerance against poisoning by CO.

A summary of the data obtained at both electrodes, Pt/GC and Pt/MWCNTs-GC is provided in Table 1.

Table 1. A summary of the electrochemical measurements extracted from Figs. 1, 3 and 4 of Pt/GC and Pt/MWCNTs-GC electrodes.

Electrode	A_r (cm²)	I_p^d / I_p^{ind}	I_p^d / I_p^b
Pt/GC	0.64	0.60	0.19
Pt/MWCNTs-GC	0.81	7.5	0.45

Since the catalyst's stability is as important as its activity, the stability of the modified electrodes was tested by recording the current as a function of time, (*i-t*), under continuous electrolysis in FA for an hour at 0.2 V. Figure 5 shows the *i-t* curves for the Pt/GC (a) and Pt/MWCNTs-GC modified electrodes (b). As expected and matching with the data of Fig. 4, the modified Pt/MWCNTs-GC electrode acquired a lower current decay with time (compare Figs. 5a and b) which means a prolonged stability during continuous electrolysis.

Overcoming CO poisoning in DFAFCs mainly proceeds through modifying the Pt with other transition metal or metal oxide that interrupt the contiguity of Pt atoms, required for adsorption of CO at Pt surface, through what is called "third body effect" and/or enhance the oxidation of CO at lower potentials through the "bifunctional mechanism" [27, 34]. In this proposed study, the enhancement in the activity and stability of the Pt/MWCNTs-GC electrodes, compared with that obtained at Pt/GC electrode, is thought to come from the unique PtNPs loading within the CNTs network minimizing its agglomeration and thus minimizing also the chance of CO adsorption at the Pt surface additionally with

the high electronic conductivity, good structural, mechanical and chemical stability and the high corrosion resistance in the fuel cell operating conditions of CNTs [35].
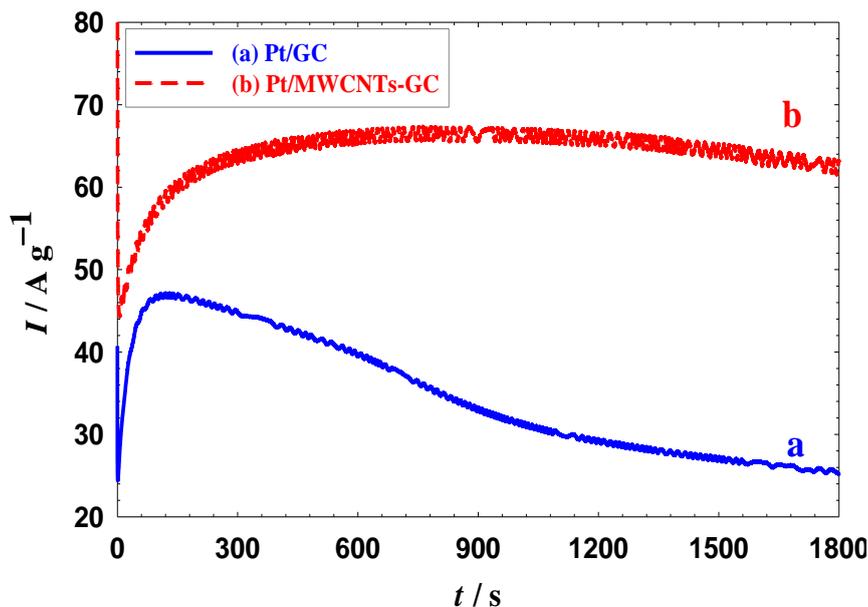
Figure 5. *i-t* curves of the (a) Pt/GC and (b) Pt/MWCNTs-GC modified electrodes measured in 0.3 M formic acid (pH = 3.5) at 0.20 V.

4. CONCLUSION

A simple modification for the GC electrode with MWCNTs is intended to enhance the catalytic activity of the direct route of FAO. The Pt/MWCNTs-GC modified electrode acquired higher I_p^d / I_p^{ind} and I_p^d / I_p^b ratios compared to the Pt/GC electrode with 12.5 and 2.3 times increase, respectively. This indicates an impressive improvement of the catalytic tolerance against poisoning by CO. Additionally, it showed a higher stability in terms of lower current decay during continuous electrolysis. The catalytic enhancement was thought to arise from minimizing the agglomeration of the PtNPs during the electrodeposition by incorporating the CNTs.

References

1. C.Coutanceau, S.Baranton, T.Audichon, Hydrogen Electrochemical Production, in: Academic Press, 2018, pp. 17.
2. J. Sun, H. Li, Y. Huang, Z. Zhuang, *Mater. Lett.*, 223 (2018) 246.
3. I.M. Al-Akraa, *Int. J. Hydrogen Energy*, 42 (2017) 4660.
4. I.M. Al-Akraa, A.M. Mohammad, M.S. El-Deab, B.E. El-Anadouli, *J. Electrochem. Soc.*, 162 (2015) F1114.

5.   I.M. Al-Akraa, A.M. Mohammad, M.S. El-Deab, B.S. El-Anadouli, *Int. J. Electrochem. Sci.*, 10 (2015) 3282.
6.   S. Curtin, J. Gangi, Fuel Cell and Hydrogen Energy Association, in: F.c.t.m. report (Ed.) Washington, D.C, 2014, pp. 1-66.
7.   H. Zhang, X. Li, X. Liu, J. Yan, *Appl. Energ.*, 241 (2019) 483.
8.   N. Matulić, G. Radica, F. Barbir, S. Nižetić, *Int. J. Hydrogen Energy*, 44 (2019) 10082.
9.   Y.-W. Rhee, S.Y. Ha, R.I. Masel, *J. Power Sources*, 117 (2003) 35.
10. X. Wang, J.-M. Hu, I.M. Hsing, *J. Electroanal. Chem.*, 562 (2004) 73.
11. N.M. Aslam, M.S. Masdar, S.K. Kamarudin, W.R.W. Daud, APCBEE Procedia, 3 (2012) 33.
12. U.B. Demirci, *J. Power Sources*, 169 (2007) 239.
13. X. Yu, P.G. Pickup, *J. Power Sources*, 182 (2008) 124.
14. A.M. Mohammad, I.M. Al-Akraa, M.S. El-Deab, *Int. J. Hydrogen Energy*, 43 (2018) 139.
15. I.M. Al-Akraa, Y.M. Asal, A.M. Mohammad, *J. Nanomater.*, 2019 (2019). Article ID 2784708.
16. Y.M. Asal, I.M. Al-Akraa, A.M. Mohammad, M.S. El-Deab, *J.Taiwan Inst. Chem. E*, 96 (2019) 169.
17. Y.M. Asal, I.M. Al-Akraa, A.M. Mohammad, M.S. El-Deab, *Int. J. Hydrogen Energy*, 44 (2019) 3615.
18. S. Hu, L. Scudiero, S. Ha, *Electrochem. Commun.*, 38 (2014) 107.
19. W.S. Jung, J. Han, S. Ha, *J. Power Sources*, 173 (2007) 53.
20. C. Rice, S. Ha, R.I. Masel, A. Wieckowski, *J. Power Sources*, 115 (2003) 229.
21. I.M. Al-Akraa, A.M. Mohammad, M.S. El-Deab, B.E. El-Anadouli, *Int. J. Electrochem Sci.*, 8 (2013) 458.
22. I.M. Al-Akraa, A.M. Mohammad, M.S. El-Deab, B.E. El-Anadouli, *Arab. J. Chem.*, 10 (2017) 877.
23. I.M. Al-Akraa, T. Ohsaka, A.M. Mohammad, *Arab. J. Chem.*, (2019).
24. I.M. Al-Akraa, Y.M. Asal, A.M. Arafa, *Int. J. Electrochem Sci.*, 13 (2018) 8775.
25. I.M. Al-Akraa, Y.M. Asal, S.D. Khamis, *Int. J. Electrochem Sci.*, 13 (2018) 9712.
26. M.S. Çögenli, A.B. Yurtcan, *Int. J. Hydrogen Energy*, 43 (2018) 10698.
27. E.N. El Sawy, P.G. Pickup, *Electrochim. Acta*, 302 (2019) 234.
28. M. Kiani, J. Zhang, Y. Luo, Y. Chen, J. Chen, J. Fan, G. Wang, R. Wang, *J. Energy Chem.*, 35 (2019) 9.
29. M.G. Abd El-Moghny, H.H. Alalawy, A.M. Mohammad, A.A. Mazhar, M.S. El-Deab, B.E. El-Anadouli, *Int. J. Hydrogen Energy*, 42 (2017) 11166.
30. G.A. El-Nagar, M.S. El-Deab, A.M. Mohammad, B.E. El-Anadouli, *Electrochim. Acta*, 180 (2015) 268.
31. G.A. El-Nagar, A.M. Mohammad, M.S. El-Deab, T. Ohsaka, B.E. El-Anadouli, *J. Power Sources*, 265 (2014) 57.
32. R. Larsen, S. Ha, J. Zakzeski, R.I. Masel, *J. Power Sources*, 157 (2006) 78.
33. J.D. Lović, A.V. Tripković, S.L.J. Gojković, K.D. Popović, D.V. Tripković, P. Olszewski, J. *Electroanal. Chem.*, 581 (2005) 294.
34. M. Choi, C.-Y. Ahn, H. Lee, J.K. Kim, S.-H. Oh, W. Hwang, S. Yang, J. Kim, O.-H. Kim, I. Choi, Y.-E. Sung, Y.-H. Cho, C.K. Rhee, W. Shin, *Appl. Catal. B: Env.*, 253 (2019) 187.
35. M. Mazurkiewicz-Pawlicka, A. Malolepszy, A. Mikolajczuk-Zychora, B. Mierzwa, A. Borodzinski, L. Stobinski, *Appl. Surf. Sci.*, 476 (2019) 806.